Chaotic synchronization in large map networks

S. H. He, H. B. Huang,* X. Zhang, Z. X. Liu, D. S. Xu, and C. K. Shen
Department of Physics, Southeast University, Nanjing 210096, China

(Received 9 April 2006; published 13 November 2006)

The chaotic synchronization in n-dimensional large map networks with local coupling and their size stabilities in the node number $N \to \infty$ are studied analytically and numerically. The analytical results show that the chaotic synchronization is stable for $N \to \infty$ in the presence of the external driving or global coupling. The numerical calculations show that, as the driving or global interaction strength increases from zero, the network states have the whole route: spatiotemporal chaotic state → cluster chaotic synchronous state → complete chaotic synchronous state → spatiotemporal pattern → spatiotemporal chaotic state.

DOI: 10.1103/PhysRevE.74.057203 PACS number(s): 05.45.Xt, 05.45.Ra, 89.75.Kd

Chaotic synchronization and pattern formation in complex networks have been the interesting research subjects in many branches of science [1–8] due to its widespread existence and applications. The main factors affecting the chaotic synchronization are the node dynamics, the coupling schemes, the coupling functions and the size of the networks. Although numerous studies have revealed some relations between the network structure and the network dynamics, the general relation are still far from being well understood. On the other hand, the size stabilities of the networks, especially the n-dimensional large map networks (nDW, $n \geq 2$) and the nonregular networks have not been clearly concerned. Only for the symmetrical local coupled regular networks were the size stabilities discussed [4,5,9]. One natural question is that under what conditions can the chaotic synchronization be stable in the limit $N \to \infty$? In general network coupling, the chaotic synchronization might be unstable in the limit $N \to \infty$. In this paper, we study the driven nDW with global and local couplings and show analytically that the chaotic synchronization is stable in the limit $N \to \infty$ for certain conditions. Numerical simulations show that with increasing the driving strength the system first enters into the cluster chaotic synchronization from the spatiotemporal chaos, then into the complete chaotic synchronization, and then into spatiotemporal pattern with a spatial wavelength of two adjacent oscillators, beyond which the system transits to spatiotemporal chaos.

The model we consider is the driven nDW with global and nearest-neighbor couplings, its dynamics is described by

$$\begin{aligned} x_{m+1}(j_1,j_2,\ldots,j_n) &= f(x_m(j_1,j_2,\ldots,j_n)) + \sum_{i=1}^{n} a_{j_i-1}[f(x_m(j_1,\ldots,j_i-1,\ldots,j_n)) - f(x_m(j_1,\ldots,j_i,\ldots,j_n))] \\ &+ \sum_{i=1}^{n} a_{j_i+1}[f(x_m(j_1,\ldots,j_i+1,\ldots,j_n)) - f(x_m(j_1,\ldots,j_i,\ldots,j_n))] \\ &+ \frac{1}{N}\sum_{\{l_i\}}^{N} d(l_1,l_2,\ldots,l_n)[f(x_m(l_1,l_2,\ldots,l_n)) - f(x_m(j_1,j_2,\ldots,j_n))] \\ &+ a_0(j_1,j_2,\ldots,j_n)[F(x_m^0) - f(x_m(j_1,j_2,\ldots,j_n))], \end{aligned} \tag{1}$$

here $f(x_m(j_1,j_2,\ldots,j_n)) = ux_m(j_1,j_2,\ldots,j_n)(1-x_m(j_1,j_2,\ldots,j_n))$ is the logistic map representing the node $(j_1,j_2,\ldots,j_n)$ chaotic dynamics, $j_i = 1,2,\ldots,N_i$ is the node index in j_i direction, $a_{j_i\pm1} \equiv a_{j_1,\ldots,j_i\pm1,\ldots,j_n}$, and $N = N_1 \times N_2 \times \cdots \times N_n$ is the nDW size. The second and the third terms in Eq. (1) describe the nearest-neighbor coupling in all directions $j_1,j_2,\ldots,j_n$, while the fourth and the last terms describe the global and driving interactions, respectively. The external drive is chosen in our present study as $F(x_m^0) = f(x_m^0) = u_0 x_m^0(1-x_m^0)$, and the periodic boundary conditions are used in the following calculations.

The synchronous state $x_m = x_m(j_1,j_2,\ldots,j_n)$, $\forall j_1,j_2,\ldots,j_n$, is described by

$$x_{m+1} = (1-a_0)f(x_m) + a_0 f(x_m^0). \tag{2}$$

In obtaining Eq. (2), we have set $a_0(j_1,j_2,\ldots,j_n) = a_0, \forall j_1,j_2,\ldots,j_n$, $d(l_1,l_2,\ldots,l_n) = d, \forall l_1,l_2,\ldots,l_n$.

*Corresponding author. Electronic address: hongbinh@seu.edu.cn

In order to study the stability of the synchronous state, we linearize Eq. (1) by defining $\Delta x_m(j_1,j_2,\ldots,j_n)=x_m(j_1,j_2,\ldots,j_n)-x_m$, let $a_{j_i\pm 1}\equiv a_i^{\pm}$ and then diagonalize the linearized equation by discrete Fourier transformation

$$\Delta x_m(j_1,j_2,\ldots,j_n)=\left(\prod_{i=1}^{n}N_i\right)^{-1/2}\sum_{\{k_i\}}\xi_m(k_1,k_2,\ldots,k_n)\times\prod_{i=1}^{n}\exp(-\sqrt{-1}2\pi j_ik_i/N_i). \tag{3}$$

The transformed variational equation is given by

$$\xi_{m+1}(k_1,k_2,\ldots,k_n)=\alpha(k_1,k_2,\ldots,k_n)f'(x_m)\xi_m(k_1,k_2,\ldots,k_n), \tag{4}$$

where $\alpha(k_1,k_2,\ldots,k_n)=1-a_0-d-\sum_{i=1}^{n}(a_i^-+a_i^+)+\sum_{i=1}^{n}(a_i^-e^{\sqrt{-1}2\pi k_i/N_i}+a_i^+e^{-\sqrt{-1}2\pi k_i/N_i})$ is an eigenvalue of the coupling matrix of the nDW, and $k_i=0,1,2,\ldots,N_i-1$. Let $a_i^{\mp}=b_i\pm c_i(c_i\leq b_i)$, where b_i and c_i are diffusive and gradient coupling parameters, respectively. We have the following Lyapunov exponent (LE):

$$\begin{aligned}\lambda(k_1,k_2,\ldots,k_n)&=\lambda_0+\ln|\alpha(k_1,k_2,\ldots,k_n)|\\&=\lambda_0+\ln\left|1-a_0-d-2\sum_{i=1}^{n}\left\{b_i\left[1-\cos\left(\frac{2\pi k_i}{N_i}\right)\right]-\sqrt{-1}c_i\sin\left(\frac{2\pi k_i}{N_i}\right)\right\}\right|,\end{aligned} \tag{5}$$

where λ_0 is the LE calculated from Eq. (2) and its linearization around the synchronous state x_m, $\lambda_0=\lim_{m\to\infty}\frac{1}{m}\sum_{l=0}^{m-1}\ln|u(1-2x_l)|$. From Eq. (5) we see that the global interaction has the same effect on the stability of the network dynamics with that of the external driving. The complete chaotic synchronization occurs if $\lambda(k_1,k_2,\ldots,k_n)<0,\forall k_1,k_2,\ldots,k_n$, that is

$$\left\{1-a_0-d-2\sum_{i=1}^{n}b_i\left[1-\cos\left(\frac{2\pi k_i}{N_i}\right)\right]\right\}^2+4\left(\sum_{i=1}^{n}c_i\sin\frac{2\pi k_i}{N_i}\right)^2<e^{-2\lambda_0}, \tag{6}$$

let $x=1-a_0-d-2\sum_{i=1}^{n}b_i\left[1-\cos\left(\frac{2\pi k_i}{N_i}\right)\right]$, and $y=2\sum_{i=1}^{n}c_i\sin\left(\frac{2\pi k_i}{N_i}\right)$, then Eq. (6) can be written as $x^2+y^2<R^2=e^{-2\lambda_0}$. The stability of the synchronous state requires that all the eigenvalues $\alpha(k_1,k_2,\ldots,k_n),\forall k_1,k_2,\ldots,k_n$, lying on the ellipses $\frac{[x-(1-a_0-d-2\sum_{i=1}^{n}b_i)]^2}{4b_i^2}+\frac{y^2}{4c_i^2}=1$, $(i=1,2,\ldots,n)$, to be contained within the circle $x^2+y^2=R^2$. For the 1DW with symmetry nearest-neighbor coupling, the stability condition was numerically studied [5], but here we give the tight bounds analytically for the chaotic synchronization in the driven nDW with global and local couplings.

If $1-a_0-d-2\sum_{i=1}^{n}b_i>0$, from Eq. (6) and the fact $c_i\leq b_i$ we see that the most unstable modes are $k_i=1$, and $N_i-1(i=1,2,\ldots,n)$, in this case the maximum size $N_{ic}(i=1,2,\ldots,n)$ that support the chaotic synchronization are determined by

$$\left\{1-a_0-d-2\sum_{i=1}^{n}b_i\left[1-\cos\left(\frac{2\pi}{N_{ic}}\right)\right]\right\}^2+4\left[\sum_{i=1}^{n}c_i\sin\left(\frac{2\pi}{N_{ic}}\right)\right]^2\lesssim e^{-2\lambda_0}, \tag{7}$$

which give the N_{ic} for different a_0, d, b_i, and c_i. In the limit $N_{ic}\to\infty$ $(i=1,2,\ldots,n)$, the stability condition becomes

$$1-a_0-d<e^{-\lambda_0}. \tag{8}$$

It is obvious that the nDW cannot be in chaotic synchronous state in the limit $N_i\to\infty$ for $\lambda_0>0$, and $a_0=d=0$.

In the case $1-a_0-d-2\sum_{i=1}^{n}b_i<0$, the most unstable modes are $k_i=\frac{N_i}{2}(i=1,2,\ldots,n)$. Now Eq. (6) becomes

$$4\sum_{i=1}^{n}b_i-(1-a_0-d)<e^{-\lambda_0}, \tag{9}$$

which is also the stability condition for chaotic synchronization in the limit $N_i\to\infty(i=1,2,\ldots,n)$. In order to determine the critical size N_{ic} analytically for different a_0, d, b_i, and c_i, we choose $k_i\approx\frac{N_{ic}}{2}\pm 1$ as the most unstable nodes, which is a good approximation for larger N_{ic}. This leads to the size equation

$$\left\{1-a_0-d-2\sum_{i=1}^{n}b_i\left[1+\cos\left(\frac{2\pi}{N_{ic}}\right)\right]\right\}^2+4\left[\sum_{i=1}^{n}c_i\sin\left(\frac{2\pi}{N_{ic}}\right)\right]^2\lesssim e^{-2\lambda_0}. \tag{10}$$

As an example, we give the critical size N_c for the driven 1DW with global and local coupling. From Eq. (7) we have

$$\sin^2\frac{\pi}{N_c}=([(1-a_0-d)b_1-2c_1^2]-\{[(1-a_0-d)b_1-2c_1^2]^2-(b_1^2-c_1^2)[(1-a_0-d)^2-e^{-2\lambda_0}]\}^{1/2})\times[4(b_1^2-c_1^2)]^{-1}\quad(b_1\neq c_1),$$

$$\sin^2\frac{\pi}{N_c}=[(1-a_0-d)^2-e^{-2\lambda_0}]\times[8b_1(1-a_0-d-2b_1)]^{-1}\quad(b_1=c_1), \tag{11}$$

while Eq. (10) leads to

$$\cos^2\frac{\pi}{N_c}=([(1-a_0-d)b_1-2c_1^2]+\{[(1-a_0-d)b_1-2c_1^2]^2-(b_1^2-c_1^2)[(1-a_0-d)^2-e^{-2\lambda_0}]\}^{1/2})\times[4(b_1^2-c_1^2)]^{-1}\quad(b_1\neq c_1),$$

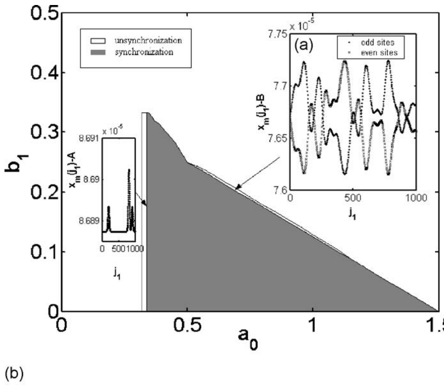

FIG. 1. Different state regions in (a_0, b_1) space for the 1DW with $u_0 = u = 4$, $c_1 = 0$, and $d = 0$. White and gray regions show the unsynchronous and synchronous states, respectively. Inset (a) shows the cluster synchronization, while inset (b) shows the spatiotemporal pattern. The constants A and B shown in the insets are determined by a_0, b_1, and initial conditions.

$$\cos^2\frac{\pi}{N_c} = [e^{-2\lambda_0} - (1 - a_0 - d)^2] \times \{8b_1[2b_1 - (1 - a_0 - d)]\}^{-1} \quad (b_1 = c_1). \quad (12)$$

In order to study the driving effect on the chaotic synchronization, we, based on Eqs. (1), (7), and (10), first simulate the dynamics of a driven 1DW with symmetrical coupling ($c_1 = 0$) and without global coupling ($d = 0$) for $u_0 = u = 4$ and different a_0, and b_1. Figure 1 shows the numerical results. If the driving constant a_0 is small, the system is in the spatiotemporal chaotic state. With increasing a_0, the system enters into cluster chaotic synchronization, inset (a) in Fig. 1 showing the $x_m(j_1)$ vs j_1. In this case, some map nodes are in complete chaotic synchronous state, and others in spatial pulse state. This pulse height and pulse number decrease as a_0 increases, finally the system enters into the complete chaotic synchronous state $x_m(j_1) = \text{constant}$, $\forall j_1$.

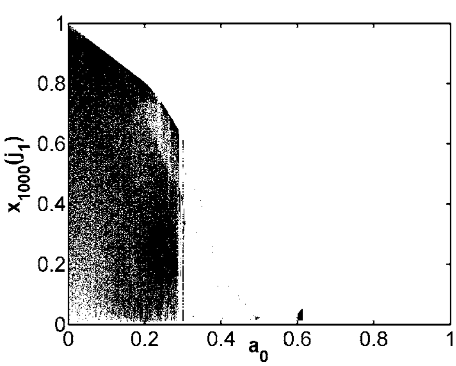

FIG. 2. Amplitude $x_{1000}(j_1)$ vs a_0 for $u_0 = u = 4$, $N = 10\,000$, $b_1 = 0.225$, $c_1 = 0$, and $d = 0$, $0 < a_0 < 0.32$, spatiotemporal chaos; $0.32 < a_0 < 0.34$, cluster synchronization; $0.34 < a_0 < 0.6$, chaotic synchronization; $0.6 < a_0 < 0.608$, spatiotemporal pattern; $0.608 < a_0$, spatiotemporal chaos.

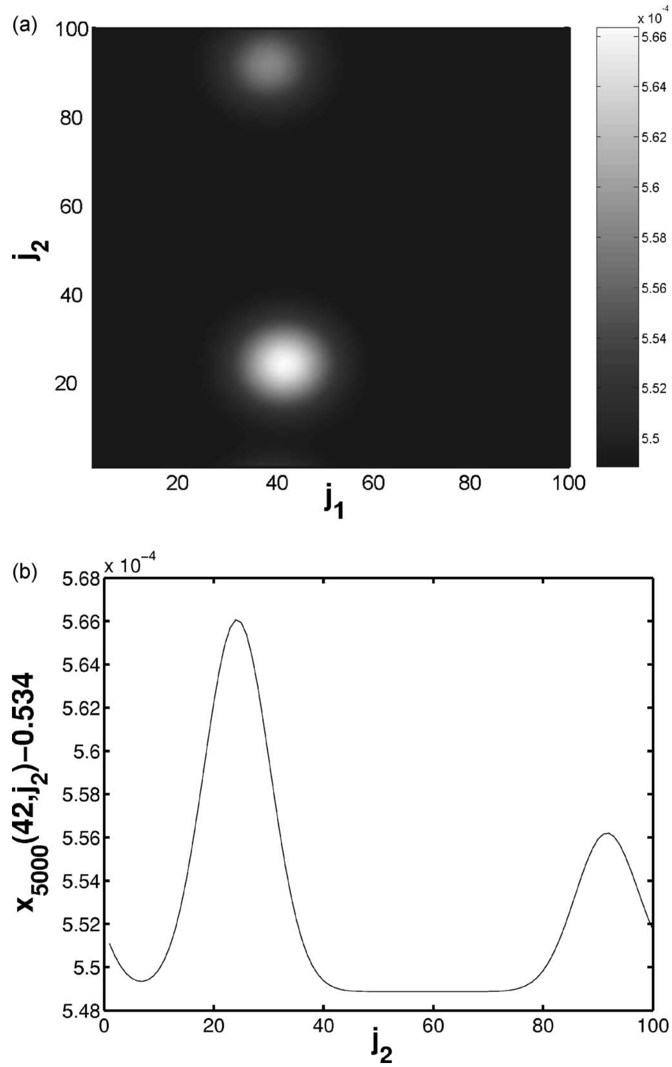

FIG. 3. (a) Plot of $x_{5000}(j_1, j_2) - 0.534$ vs j_1 and j_2 for the 2DW, which shows the cluster synchronization. The network size $N_1 \times N_2$ is 100×100, and the parameters are $u_0 = u = 4$, $d = 0$, $b_1 = 0.11$, $b_2 = 0.12$, $c_1 = -0.1$, $c_2 = 0.1$, and $a_0 = 0.324\,33$. (b) Plot of $x_{5000}(42, j_2) - 0.534$ vs j_2, the parameters are the same as (a).

Further increasing a_0, the synchronous state $x_m(j_1) = \text{constant}$ loses the stability to a state of the form $x_m(j_1) = \text{constant} + (-1)^{j_1} \cdot \text{amplitude}$, for $0.1 < b_1 < 0.25$ [see inset (b)]. This spatial pattern has a spatial wavelength of two nodes [10], and the *amplitude* of $x_m(j_1)$ increases with increasing a_0, and finally the system enters into the spatiotemporal chaotic state. However, in the regions $b_1 > 0.25$ and $b_1 < 0.1$, this spatiotemporal pattern disappears, and the system transits to the spatiotemporal chaotic state from synchronous state abruptly. Figure 2 shows the relation $x_{1000}(j_1) - a_0$ for $u_0 = u = 4$, $N = 10\,000$, $b_1 = 0.225$, and $c_1 = d = 0$, which reflects the whole route discussed above. The similar case occurs for the driven nDW with asymmetrical local coupling ($c_1 \neq 0$). Figures 3 and 4 show the typical cluster synchronization and spatiotemporal pattern for the 2DW with $u_0 = u = 4$, $d = 0$, $b_1 = 0.11$, $b_2 = 0.12$, $c_1 = -0.1$, and $c_2 = 0.1$, respectively.

In the above discussions, we have let $a_0(j_1, j_2, \ldots, j_n)$

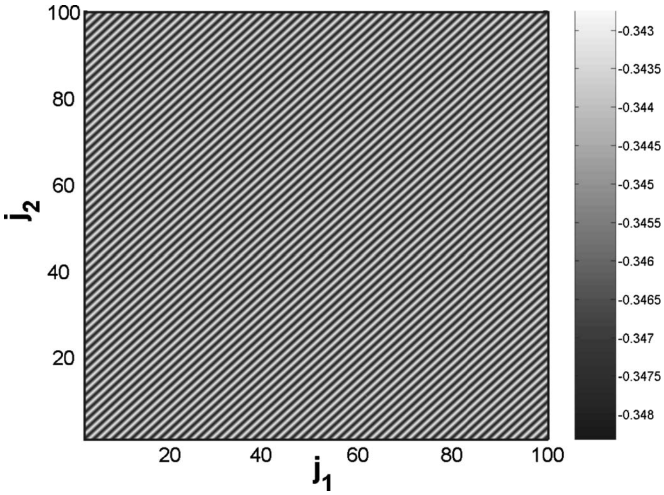

FIG. 4. Plot of $x_{5000}(j_1,j_2)$ vs j_1 and j_2 for the 2DW, which shows the spatiotemporal pattern. The network size is 100×100, and the parameters are $u_0=u=4$, $d=0$, $b_1=0.11$, $b_2=0.12$, $c_1=-0.1$, $c_2=0.1$, and $a_0=0.581$. It clearly shows that the neighboring nodes have the opposite phase.

$=a_0, \forall j_1,j_2,\ldots,j_n$ and $d(l_1,l_2,\ldots,l_n)=d, \forall l_1,l_2,\ldots,l_n$, that is all nodes have the same driving and global couplings. An interesting phenomenon that should be noted is that the synchronous state $x_{m+1}=[1-a_0(j_1,j_2,\ldots,j_n)]f(x_m)+a_0(j_1,j_2,\ldots,j_n)f(x_m^0)$ is not sensitive to the coupling symmetry, the chaotic synchronization also occurs if the coupling constants $a_{j_i\pm 1}$, $d(l_1,l_2,\ldots,l_n)$ and (or) $a_0(j_1,j_2,\ldots,j_n)$ are different for different j, i, and l. For example, for the 1DW with $d(l_1)=0, N=10\,000$, the chaotic synchronization also occurs if all $a_{j_1\pm 1}(j_1=1,2,\ldots,N)$ are random numbers chosen from the region $[0,0.1]$ of uniform distribution and all $a_0(j_1)(j_1=1,2,\ldots,N)$ are random numbers chosen from the region $[0.55,1]$ of uniform distribution. But in this case only spatiotemporal and synchronous chaotic states exist, the cluster synchronization and spatiotemporal pattern disappear.

It should be stressed that the global coupling has the similar effect on the dynamics of the nDW to that of the external driving.

In summary, we have given the analytical conditions for chaotic synchronization in both finite size and the infinite size $(N\to\infty)$ of the driven nDW. Numerical calculation shows that the transitions between the chaotic synchronization and the spatiotemporal chaos is via cluster chaotic synchronization, or the spatiotemporal pattern with the neighboring nodes having opposite phase (π), or the crisis.

This work was supported by NSF of Jiangsu province (Grant No. BK2005062).

[1] S. Boccaletti, J. Kurths, G. Osipov, D. L. Valladares, and C. S. Zhou, Phys. Rep. **366**, 1 (2002); S. Boccaletti, V. Latora, Y. Moreno, M. Chavez, and D.-U. Hwang, *ibid.* **424**, 175 (2006).
[2] T. Fukuyama, R. Kozakov, H. Testrich, and C. Wilke, Phys. Rev. Lett. **96**, 024101 (2006).
[3] M. G. Cosenza, M. Pineda, and A. Parravano, Phys. Rev. E **67**, 066217 (2003); S. Jalan and R. E. Amritkar, Phys. Rev. Lett. **90**, 014101 (2003).
[4] P. Palaniyandi, P. Muruganandam, and M. Lakshmanan, Phys. Rev. E **72**, 037205 (2005).
[5] M. Pineda and M. G. Cosenza, Phys. Rev. E **71**, 057201 (2005).
[6] K. Kaneko, Phys. Rev. Lett. **69**, 905 (1992).
[7] I. Aranson, D. Golomb, and H. Sompolinsky, Phys. Rev. Lett. **68**, 3495 (1992).
[8] C. Masoller and A. C. Martí, Phys. Rev. Lett. **94**, 134102 (2005).
[9] L. M. Pecora, Phys. Rev. E **58**, 347 (1998); M. Barahona and L. M. Pecora, Phys. Rev. Lett. **89**, 054101 (2002).
[10] J. P. Crutchfield and K. Kaneko, *Directions in Chaos*, edited by Bai-lin Hao (World Scientific, Singapore, 1987).